Assiut Univ. J. of Physics *Printed ISSN 1687-4900*
47(2), p-p 41-53(2018)

Investigation of ^{6}Li+^{24}Mg Elastic Scattering Using Different Folding Models

Sherif R. Mokhtar[1, *], Awad A. Ibraheem[2,3], Eman Abdel-Rahman[1] and M. El-Azab Farid[1]

[1] *Physics Department, Assiut University, Assiut 71516, Egypt*
[2]*Physics Department, King Khalid University, Abha, Saudi Arabia*
[3]*Physics Department, Al-Azhar University, Assiut Branch, Assiut 71524, Egypt*

Email:[*]*srmokhtar@yahoo.com*

Accepted: 10/9/2018 **Received:** 16/9/2018 **Available Online:**20/12/201

In the present study we investigate the ^{6}Li+^{24}Mg elastic scattering at two energies 88 and 240 MeV in the framework of the optical model. Two optical real potentials are used here, according to α-cluster structure of the colliding nuclei. The first double folding (DF) potential for the real central part of the nuclear optical potential is done by folding the α-n and α-α effective interactions between target and projectile nuclei over the density distributions of α-clusters in the target (^{24}Mg) nucleus and considering the α-deuteron (α-D) structure of the projectile (^{6}Li) nucleus. We call this one is double folding cluster (DFC). The Second potential is DF optical potentials based upon the São Paulo (SP) potential. The imaginary part of the optical potential is calculated in the Woods-Saxon form (WS) for DFC, while for SP both imaginary WS and imaginary folded potentials are used. The experimental angular distributions of the elastic scattering data are successfully obtained using the derived potential. It is found that introducing a real renormalization factor, N_R, smaller than unity is essential in order to obtain successful description of the data. The obtained values of N_R in case of SP are more close to unity than those of DFC. The obtained results confirm the validity of the SP to generate nucleus-nucleus optical potentials.

Keywords: Optical model; Elastic scattering; Folding potential; Cluster model; São Paulo potential

PACS: 25.70.Bc; 24.10.Ht; 27.20.+n. ;21.60.Gx

I. INTRODUCTION

The optical model is one of the mostly used models for the description of nuclear scattering especially elastic scattering. The microscopic description of the nucleus–nucleus optical model potential is considered as one of the fundamental tasks in nuclear reaction physics. One of the used methods to

derive the nucleus-nucleus interaction potential is the folding model. The pioneered folding work of Watanabe in his analysis of deuteron projectiles is considered as a review article of this model [1]. In the last few decades, folding model calculations, with microscopic and semi microscopic approaches, were used for the analysis of scattering processes for a large number of interacting systems. Satchler and Love [2,3] have been successfully used M3Y double folding (DF) model for the analysis of light and heavy composite ions scattering. In their analysis, DF optical potential was built on a realistic effective nucleon–nucleon (NN) interaction folded with the nuclear matter density distributions of projectile and target nuclei. The DF model based on matter densities and on the effective NN interaction is successfully used to analyze α-nucleus and nucleus-nucleus elastic scattering [4-9]. The elastic scattering of ^{6}Li and ^{9}Be projectiles were exceptions where the folded potential must be reduced by a renormalization coefficient (~0.5–0.6) [2, 10-12]. Many studies have been carried out on the scattering of ^{6}Li which have distinguished interest. ^{6}Li ion falls in the mass range A = 4 - 12 of ions whose elastic scattering exhibits a transition [13] between characteristic of light ions (A≤4) and those of heavy ions (A≥ 12). On the other hand, it is commonly surmised that, because ^{6}Li is weakly bound (1.47 MeV for ^{6}Li →α+D), breakup has a large effect on the elastic scattering channel and is responsible for the reduction of the renormalization factor below unity. In our previous study [14] we performed analysis of ^{6}Li+^{28}Si scattering at low energies (9-20 MeV) by employing the α-cluster structure of the colliding nuclei in order to generate semi-microscopic DF potentials considering different targets. In the present work we extend our calculations to analyze ^{6}Li+^{28}Mg scattering at the two available energies 88 and 240 MeV which are relatively higher energies than those considered previously [14]. In the same time, for the sake of comparison, the considered scattering data are reanalyzed using a microscopic SP potential. So, the present work represents an extension of our previous studies [14-16] in order investigate the validity of α-cluster structure of colliding nuclei to construct semi-microscopic folding nucleus-nucleus potentials. The manuscript is organized as follows: in the next section the theoretical formalism is presented, while calculations procedure is given in section III. Results and disscussion are demonstrated in section IV and finally conclusions are summarized in section V.

II. FORMALISM

II.1. The semi-microscopic DF cluster model

Considering the α-D cluster structure of ^{6}Li nucleus, the ^{6}Li+nucleus semi-microscopic DF potential can be written as [14].

$$V_{^{6}Li-Target}^{DFC}(R) = \int |\Psi(Z)|^2 \left[V_{\alpha-Target}\left(\left|\vec{R} - \tfrac{1}{3}\vec{Z}\right|\right) + V_{D-Target}\left(\left|\vec{R} + \tfrac{2}{3}\vec{Z}\right|\right)\right] d\vec{Z} \quad (1)$$

where R is the separation distance between the centers of projectile and target nuclei and Z is the α–D separation distance inside ^{6}Li nucleus. Ψ(Z) is the wave function of the relative motion of alpha and D clusters in the ground state of ^{6}Li nucleus. The relative wave function of ^{6}Li can be expressed as [17]

$$\Psi(\mathbf{Z}) = \frac{\mathbf{4\beta}}{\sqrt{\mathbf{15}}}\left(\frac{\mathbf{2\beta}}{\boldsymbol{\pi}}\right)^{\mathbf{3/4}} \mathbf{Z^2}\,\mathbf{exp}(-\boldsymbol{\beta}\mathbf{Z^2}),\ \boldsymbol{\beta} = \mathbf{0.11\ fm^{-2}} \quad (2)$$

So, considering the α-cluster structure of target nucleus, we can formulate the α+target single folding potential as

$$\mathbf{V_{\propto-Target}(r)} = \int \boldsymbol{\rho}_{\mathbf{CTarget}}(\grave{\mathbf{r}})\, \mathbf{V}_{\propto-\propto}\left(\left|\vec{\mathbf{r}} - \vec{\grave{\mathbf{r}}}\right|\right) \mathbf{d}\vec{\grave{\mathbf{r}}}\ \ \mathbf{MeV}\ , \quad (3)$$

where $\boldsymbol{\rho_{CTarget}}$ is the α-cluster distribution density inside the target nucleus. Adopting the composition: ^{24}Mg≡6α, the α-cluster density distribution of the target can be represented in the harmonic oscillator (HO) form as

$$\boldsymbol{\rho_c(r)} = \boldsymbol{\rho_{0c}}(\mathbf{1} + \boldsymbol{\mu}\,\boldsymbol{r^2})\ \mathbf{exp}(-\boldsymbol{\xi}\boldsymbol{r^2}), \quad (4)$$

with the parameters ρ_{0c}, μ and ξ equal to 0.0502 fm^{-3}, 0.6002 fm^{-2} and 0.3173 fm^{-2}, respectively. This density has a root mean square (rms) radius of 3.048 fm. The $\propto -\propto$ interaction, $V_{\propto-\propto}$, is represented in the Gaussian form as:

$$V_{\propto-\propto}(s) = -V_{0\propto}\, exp(-\kappa\, s^2)\ \text{MeV}\ . \quad (5)$$

Similarly, the D–Target interaction potential can be formulated as:

$$\boldsymbol{V_{D-Target}(r)} = \int \boldsymbol{\rho_{CTarget}}(\grave{\boldsymbol{r}})\, \boldsymbol{V}_{\mathbf{D}-\propto}\left(\left|\vec{\boldsymbol{r}} - \vec{\grave{\boldsymbol{r}}}\right|\right) \boldsymbol{d}\vec{\grave{\boldsymbol{r}}}\ \ \mathbf{MeV}\ , \quad (6)$$

where the D–α interaction can be expressed in the form:

$$\boldsymbol{V_{\mathbf{D}-\alpha}(r)} = \mathbf{2}\int |\boldsymbol{\varphi}(\boldsymbol{Y})|^{\mathbf{2}}\, \boldsymbol{V}_{\mathbf{n}-\propto}\left(\left|\vec{\boldsymbol{r}} + \vec{\boldsymbol{Y}}\right|\right)\boldsymbol{d}\vec{\boldsymbol{Y}}\ \ \mathbf{MeV}\ , \quad (7)$$

where $\varphi(Y)$ is the wave function of the proton–neutron relative motion inside the deuteron. If we ignore the d-state we can assume the s-state wave function to be [18]

$$\boldsymbol{\varphi(Y)} = \left(\frac{\mathbf{2}\boldsymbol{\lambda}}{\boldsymbol{\pi}}\right)^{\mathbf{3}/\mathbf{4}} \mathbf{exp}(-\boldsymbol{\lambda}\boldsymbol{Y^2}),\ \boldsymbol{\lambda} = \mathbf{0.053\ fm^{-2}}\ . \quad (8)$$

The α–nucleon (α–n) interaction, $V_{\alpha-n}$, is taken in a Gaussian form as [19].

$$\mathrm{V_{n-\propto}(s)} = -\mathrm{V_{0n}}\exp(-\chi\, s^2)\ \text{MeV} \quad (9)$$

Table I. Parameters of the α−α and n−α effective interactions used in Eqs.(5,9)

Interaction	V_{0n} ($V_{0\alpha}$) (MeV)	χ (κ) ($\mathbf{fm^{-1}}$)
α−α	122.62	0.469
n−α	36.4	0.2657

II.2. The São Paulo potential

Several theoretical potential models have been developed to account for the energy dependence. One of them associates this dependence with nonlocal quantum effects related to the exchange of nucleons between target and projectile [20-22]. It is a global parameter-free optical potential known as the São Paulo optical potential. The SP potential has been successfully used to describe the elastic scattering and peripheral reaction channels for a large number of heavy-ion systems in a very wide energy region, from sub-Coulomb to 200 MeV/nucleon [23-40] .It has been also used to describe the total reaction and fusion cross sections for hundreds of systems [20-22]. Through this model, the bare interaction V_N is correlated to the folding potential V_F as

$$\mathbf{V_N(R,E) = V_F(R)\exp(-4v^2/c2)} \quad , \qquad (10)$$

where c is the speed of light and **v** is the local relative velocity between the two colliding nuclei. So the total nucleus-nucleus potential can be expressed as

$$\mathbf{V^2(R,E) = \frac{2}{\mu}[E - V_c(R) - V_N(R,E)]} \qquad (11)$$

where V_c is the Coulomb potential. The velocity-dependence of the potential arises from the effects of the Pauli non-locality [23,41]. The SP potential is obtained numerically by solving Eqs. (10,11) through an iterative process. The folding potential depends on the matter densities of the colliding nuclei as

$$\mathbf{V_F(R) = \int \rho_1(\vec{r}_1)\rho_2(\vec{r}_2)V_0\delta(\vec{R} - \vec{r_1} + \vec{r_2})d\vec{r_1}\, d\vec{r_2}} \qquad (12)$$

with V_0 = 456 MeV fm^3. The use of the matter densities and delta function in Eq. (12) corresponds to the zero-range approach for the folding potential, which is equivalent [42] to the more usual procedure of using an effective nucleon-nucleon (NN) interaction with the nucleon densities of the nuclei (instead of the matter densities). We considered the two-parameter Fermi (2pF) distribution to describe the nuclear densities

$$\boldsymbol{\rho(r)=\frac{\rho_0}{1+\exp\left(\frac{r-R_0}{a}\right)}} \qquad (13)$$

The radii of the matter (ρ_{0M}) and charge (ρ_{0C}) densities can be well represented using $R_{0M} = 1.31A^{1/3} - 0.84$ fm and $R_{0C} = 1.76\ Z^{1/3} - 0.96$ fm, respectively. The charge and matter distributions present average diffuseness values of $a = 0.53$ fm and $a = 0.56$ fm, respectively. The SP potential is based on the systematic of the nuclear densities. The average diffuseness value of this systematic is $a = 0.56$ fm. As already commented, small deviations around this average value are expected due to the effects of the structure of the nuclei. In Ref.[42] these variations were analyzed and a standard deviation of $\Delta = 0.025$ fm was found. A realistic value for the diffuseness should not be too far from the average value. For the imaginary part of the optical potential, the code can work with two models. It can use a Woods-Saxon (WS) shape or $W(R) = N_I\, V(R)$. The WS potential has the 3-parameter form $W(R) = W_0\, f_i(R)$,

$$\boldsymbol{f_i(R) = \left[1 + \exp\left(\frac{R - Ri}{ai}\right)\right]^{-1}}. \quad \mathbf{R_i = r_i A^{1/3}} \qquad (14)$$

The latter model has been applied for several systems in a wide energy range (see Ref.[33]). It was found that the average normalization value $N_I = 0.8$ works very well for most of considered scattering systems.

III. PROCEDURE

To analyze the ^{6}Li+^{24}Mg elastic scattering data at 88 MeV [43] and at 240 MeV [44], we use the DF optical potential generated from the Eqs. (1, 10) considering the following procedure:

1) We neglected the spin-orbit potential since it is well known that elastic scattering cross section data in this energy range are not sensitive to this potential [2].

2) The considered sets of data are analyzed using the DFC expressed by Eq. (1) and four versions of the folded optical SPP (Eq. (10)) denoted as OM1, OM2, OM3 and OM4. The OM1 potential represents only the real part of the interaction (10) and the projectile and target densities taken in 2PF form from SPP while the imaginary part of the optical potential is phenomenologically parameterized in a WS form (14). The OM2 is the same as OM1 but the imaginary part is taken in the folded form (10) normalized by the factor N_I. The OM3 is the same as OM1 but considering the following form [45] of nuclear matter density of ^{6}Li instead of the 2pF form.

$$\rho_P^{^6Li}(r_1) = 0.203 \exp(-0.3306\ r_1^2) + (-0.0131 + 0.001378\, r_1^2) \exp(-0.1584\, r_1^2)\ \text{fm}^{-3} \qquad (15)$$

The OM4 is the same as OM2 but using the density (15).

3) The obtained potentials are fed into the computer code HIOPTIM-94 [46] to compute the elastic scattering differential cross sections.
4) Routine searches are performed on four free parameters (N_R besides the WS imaginary potential parameters W, r_I and a_I for the OM1 and OM3 while two free parameters (the real and imaginary renormalization factors N_R and N_I) are searched on for the OM2 and OM4 potentials in order to minimize the chi-squared χ^2, defined as

$$\chi^2 = \frac{1}{N_D}\sum_{k=1}^{N_D}\left[\frac{\sigma_{th}(\theta_k)-\sigma_{exp}(\theta_k)}{\Delta\sigma_{exp}(\theta_k)}\right]^2 \qquad (16)$$

where σ_{th} and σ_{exp} are the theoretical and the experimental differential cross section, respectively, at the angle θ_K, N_D is the number of angles at which measurements are performed and $\Delta\sigma_{exp}(\theta_k)$ is the error associated with $\sigma_{exp}(\theta_k)$.

IV. RESULTS AND DISCUSSION

The best fit parameters extracted from the auto search using the HIOPTM-94 code from the derived DFC and SP potentials for the considered elastic scattering data are listed in Tables II and III, respectively. The parameters of the phenomenological WS optical potentials, the corresponding real and imaginary volume integrals per interacting nucleon pair; J_R and J_I and the absorption (reaction) cross sections σ_R are also shown. The resulting angular distributions of the elastic scattering differential cross section using the generated real DFC and all types of SP potentials, in conjunction with imaginary WS potentials are shown in Figs.1 and 2 in comparison with the corresponding experimental data.

It is shown that in order to obtain successful reproduction of the data it is necessary to introduce a reducing renormalization factor N_R is far from unity (0.537 for 88 MeV and 0.676 for 240 MeV) for the assumed depths of the considered α-α and α-n effective interactions defined by the parameters listed in Table I. In case of SP potential the renormalization factor N_R is modified and becomes more close to unity for all considered OM types. It is noticed from Figs. 1 and 2 that the extracted predictions of the data using the both derived real semi-microscopic DFC and microscopic SP potentials supplemented by phenomenological imaginary WS potentials (denoted as OM1) are almost identical all over the measured angular ranges. It is noticed from Figs. 1 and 2 and the values of χ^2 shown in Tables II and III that fits with data obtained using DFC, OM1 and OM3 potentials are better than those resulted using OM2 and OM4 potentials. This may be attributed to the more flexibility of the supplemented imaginary phenomenological WS potentials supplemented for

the DFC, OM1 and OM3 potentials based upon three free parameters while in OM2 and OM4 potentials there is only one free parameter considered in the search of folded imaginary potentials. So, the following discussion is restricted to DFC and SP (OM1) only.

Figure 3 presents a comparison between the derived DFC and SP (OM1) renormalized real potentials. It is noticed from the figure that the DFC potentials are apparently deeper than the corresponding SP ones inside the interior region (at small radii). It is observed also from the figure that the consistency between the DFC and SP potentials moves toward the surface region (at larger radii) with increasing the bombarding energy. This indicates that the elastic scattering cross section of the considered reaction is clearly insensitive to the strength (amplitude) of the nuclear potential at small radial distances and the sensitivity is confined to the surface region The resulting imaginary volume integrals J_I and the absorption (reaction) cross section, σ_R deduced for ^{6}Li+ ^{24}Mg system using the DFC and SP potentials are listed in Tables II and III

Finally, regarding the resulted values of the renormalization factor, N_R, for the constructed DFC and SP(OM1) potentials listed in Tables II and III, respectively, one may notice that for the DFC potential needs to be normalized with reducing factor which goes down lower than unity. As for the SP potential, it is clearly noted that N_R value is better than those of DFC potential.

So, from the investigation of the present results and those of our previous study one may extract a confirmation that the generated DFC potential is able without renormalization to successfully reproduce ^{6}Li elastic scattering data at relatively low bombarding energies. At higher energies, DFC potential needs a renormalization of about 0.6 ± 0.05. On the other side, the present results provide an additional evidence for the ability of the SPP to successfully describe ^{6}Li elastic scattering with renormalization close to unity and similar to work of [44]. In Ref. [44], the authors used density dependent version of M3Y interaction called CDM3Y6. However, in the same time, the present results indicate that the constructed standard SP potential [20-22] needs to be renormalized by a reducing factor in order to produce successful predictions of the data at higher energies.

V. SUMMARY AND CONCLUSIONS

The present work is directed to analyze ^{6}Li+^{24}Mg elastic scattering in the framework of DF optical model based upon the α-cluster. The derived DF potentials are considered as the real part of the nuclear optical potentials. The imaginary part is treated phenomenologically through the WS form in order to analyze the elastic scattering differential cross section of experimental data in

the considered energy range. Successful description of the data is obtained with the derived semi-microscopic DFC real potentials.

For the sake of comparison, the same elastic scattering data are reanalyzed using microscopic SP potentials. It is found that although the DFC and SP potentials are generated in the framework of different folding approaches based upon different ingredients (matter densities and effective interactions) they produce similar predictions of the data all over the measured angular ranges. So, the results of the present work provide an additional evidence that the α-cluster structure can be successfully used to construct semi-microscopic nuclear potentials for light heavy nuclei. While SP potential is a good candidate for describing the data with better results than those of CDM3Y6 and DFC potentials[47,48].

Finally, it is worthwhile to point out that our previous and present analysis reveal a considerable confirmation of the substantial ability of the DFC potentials to reproduce elastic scattering data for light heavy nuclei. The cluster model was successfully used to describe many reactions such as α $+^{40}$Ca [49]. Therefore, it is greatly recommended to perform more investigations on the analysis of elastic and inelastic scattering and other nonelastic channels using the DFC potential. The extension of this work to other energies and targets is important to complete the picture. Recently, elastic scattering of ^{6}Li+^{28}Si at seven energies in the energy range from 76 to 318 MeV is prepared to be published. While, elastic scattering of ^{6}Li+^{40}Ca at nine energies in the energy range from 26 to 240 MeV is submitted to [50]. In the same time SP is

Table II. Best fitting parameters obtained for ^{6}Li +^{24}Mg elastic scattering using the DFC potential.

E_{Lab} MeV	N_R	W_0 MeV	r_I fm	a_I fm	J_R MeVfm^3	J_I MeVfm^3	σ_R mb	χ^2
88	0.537	8.291	1.5636	0.7929	214.16	117.86	1664	11.40
240	0.676	34.523	0.9317	1.2276	269.84	149.98	1962	9.05

Table III. Same as Table III but using the SP model.

E_{Lab} MeV	Potential Shape	W_D MeV	N_R	W_0 MeV	r_I fm	a_I fm	J_R MeVfm^3	J_I MeVfm^3	σ_R mb	χ^2
88	OM1	27.14	0.785	1.546	1.1904	1.0206	275.89	149.81	1899	19.74
	OM2		0.697	1.258	-	-	244.80	353.59	1567	82.88
	OM3	2.560	0.699	156.88	1.0693	0.9658	258.48	275.28	1800	21.96
	OM4		0.642	1.089	-	-	237.16	332.38	1618	34.51
240	OM1		0.831	34.518	0.9599	1.0219	240.89	139.05	1664	6.33
	OM2		0.996	1.459	-	-	288.82	338.41	1464	16.12
	OM3		0.935	53.482	0.9089	0.9171	285.25	176.63	1591	4.50
	OM4		0.984	1.307	-	-	300.17	318.96	1509	13.01

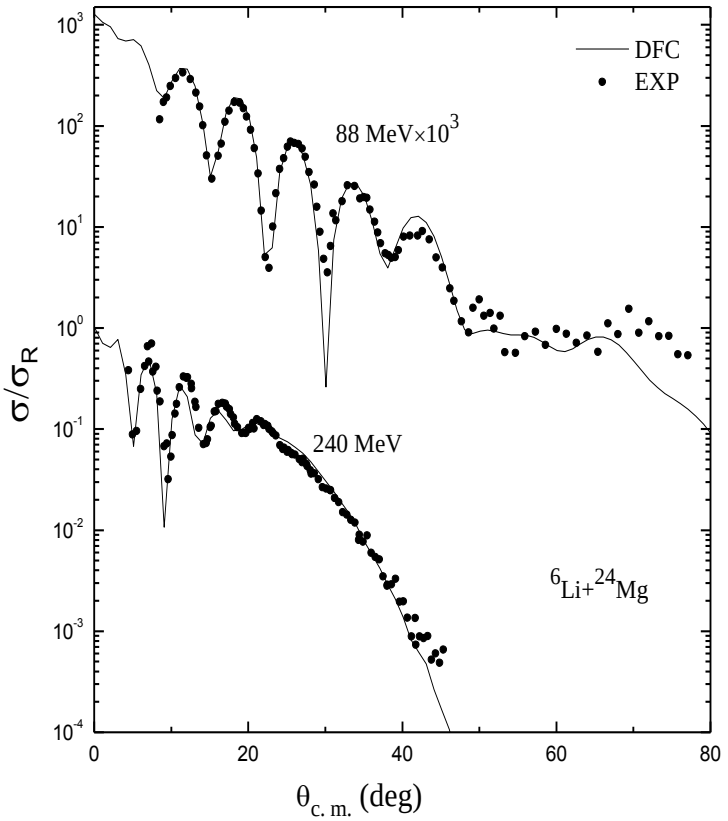

Fig. 1 ^{6}Li+^{24}Mg elastic scattering using the DFC potential extracted from expressions (1) in comparison with experimental data.

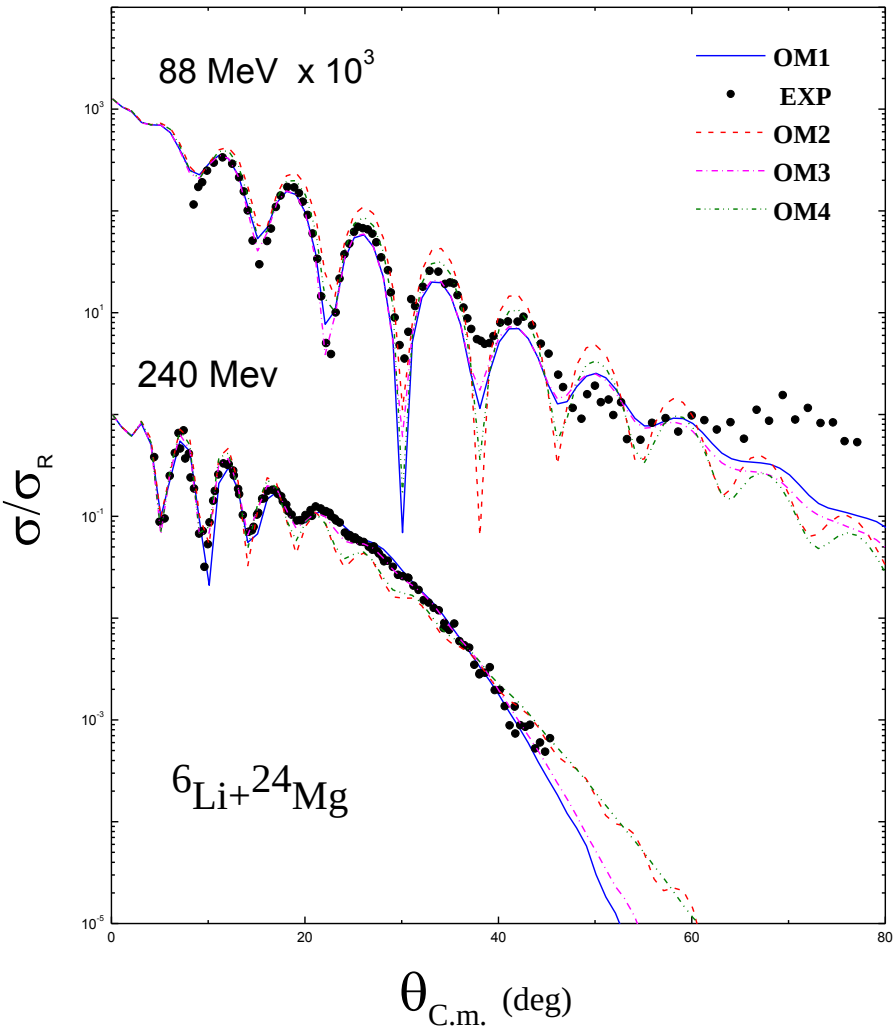

Fig. 2 $^{6}Li+^{24}Mg$ elastic scattering using the SP potential extracted from expressions (10) in comparison with experimental data.

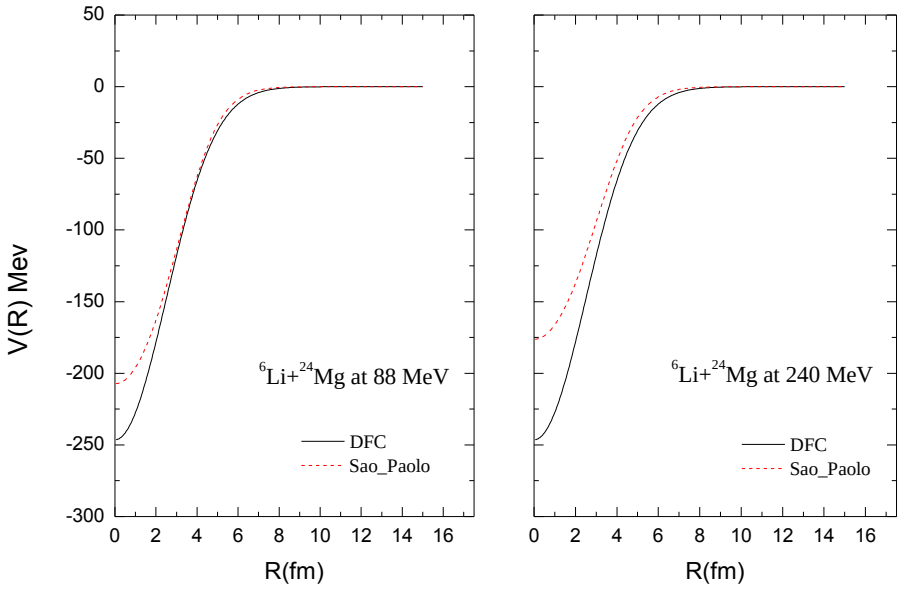

Fig. 3: A comparison between the derived real nornalized DFC and SP potentials.

Reference

[1] S. Watanabe, Nucl. Phys. **8**, 484(1958).

[2] G. R. Satchler and W. G. Love, Phys. Rep. **55**, 183 (1979).

[3] M. E Brandan and G. R. Satchler, Phys. Rep. **285**, 143 (1997).

[4] D. T. Khoa, W. Von Oertzen, H. Bohlen, and F. Nuoffer, Nucl.Phys. **A 672**, 387 (2000).

[5] T. Furumoto, and Y. Sakuragi, Phys. Rev. C**74**, 034606(2006).

[6] S. Ohkubo, Y. Hirabayashi, J.Phys. Conference Series **11**, 012014 (2008).

[7] W. Zou, Y. Tian, and Z.-Y. Ma, Phys. Rev. C **78** , 064613 (2008).

[8] T. L. Belyaeva, *et al*, Phys.Rev. C **82**, 054618 (2010).

[9] Y. Hirabayashi and S. Ohkubo, Phys. Rev. C **88** , 014314 (2013).

[10] M. El-Azab Farid and M. A. Hassanain, Nucl. Phys. **A 678**, 39 (2000).

[11] D. T. Khoa, G. R. Satchler, and W. von Oertzen, Phys.Rev. C **51**, 2069 (1995).

[12] Y. Sakuragi, Phys. Rev. C**35**,2161(1987); Y.Sakuragi , M.Yahiro and M. Kamimura, Prog. Theor. Phys. Suppl. **89**, 36 (1986); Y.Sakuragi *et al*, Prog. Theor. Phys. **98,** 521(1997).

[13] R. M. DeVries, D. A. Goldberg and J. W. Watson *et al*, Phys. Rev.Lett. **39**, 450 (1977).

[14] M. El-Azab Farid, A. A Ibraheem and J H Al-Zahrani *et al*, J. Phys. **G 40**, 075108 (2013).

[15] A. H. Al-Ghamdi , Awad A. Ibraheem and M. El-Azab Farid; *Commun. Theor. Phys.* 58 135 (2012)

[16] M. A. Hassanain, Awad A. Ibraheem, and M. El-Azab Farid; Phys. Rev. C **77**, 034601(2008) .

[17] K. H. Bray *et. Al.* Nucl. Phys. **A 198** , 129 (1972).

[18] A.Y. Abul-Magd and M. El-Nadi, Prog. Theor. Phys. **35** , 798 (1966).

[19] V. G. Neudatchin *et al*, Phys. Lett. **B 34**, 581 (1971).

[20] L. R. Gasques *et al*, Nucl. Phys. **A 764**, 135 (2006).

[21] L. R. Gasques *et al*, Phys. Rev. C **69**, 034603 (2004)

[22] L. C.Chamon *et al*, Prog. Theor. Phys. Supp **154**, 169 (2004).

[23] L. C. Chamon *et al*, Phys. Rev. Lett. **79**, 5218 (1997).

[24] J. J. S. Alves, *et al*,Nucl. Phys. **A 748** , 59 (2005) .

[25] D. Pereira *et al*, Phys. Rev.C **73**, 014601 (2006).

[26] L. C. Chamon, D. Pereira, and M. S. Hussein, Phys. Rev. C **58,** 576 (1998).

[27] M. A. G. Alvarez *et al*, Nucl. Phys. **A 656**, 187 (1999).

[28] L. R. Gasques *et al*, Phys. Rev. C **65**, 044314 (2002).

[29] E. S. Rossi Jr. *et al*, Nucl. Phys. **A 707**, 325 (2002).

[30] L. R. Gasques *et al* Phys. Rev. C **67**, 024602 (2003).

[31] T. Tarutina , L. C. Chamon and M. S. Hussein, Phys. Rev. C **67**, 044605 (2003).

[32] L. C. Chamon, Nucl. Phys. **A 787**, 198 (2007).

[33] M.A.G.Alvarez *et al*, Nucl. Phys. **A 723**, 93 (2003).

[34] L. R. Gasques *et al*, Phys. Rev. C **67,** 067603 (2003).

[35] P. R. S. Gomes *et al*, Phys. Rev. C **70**, 054605 (2004).

[36] M. A. G. Alvarez *et al*, Nucl. Phys.**A 753**, 83 (2005).

[37] P. R. S. Gomes *et al*, Phys. Rev. C **71**, 034608 (2005).

[38] J. J. S. Alves *et al*, Braz. J. Phys. **35**, 909 (2005).

[39] P. R. S. Gomes *et al*, J. Phys. **G** 31, S1669. (2006).

[40] P.R.S. Gomes *et al*, Phys. Lett. **B 634**, 356 (2006).

[41] M. A. Cândido Ribeiro *et al*, Phys. Rev. lett. **78**, 3270 (1997).

[42] L. C. Chamon *et al*, Phys. Rev. C **66**, 014610 (2002).

[43] C. Fulmer, G. R. Satchler, E. E. Gross, F. E. Bertrand, C. D. Goodman, D. C. Hensley, J. R. Wu, N. M. Clarke, and M. F. Steeden,Nucl. Phys. **A 356**, 235 (1981).
[44] X. Chen, Y.-W. Lui, H. Clark, Y. Tokimoto, and D. H. Youngblood,Phys. Rev. **C 80**, 014312 (2009).
[45] K. Bray, K. Jayaraman, G. Lobianco, G. Moss, W. Van Oers, D. Wells, and F. Petrovich,Nucl. Phys. **A 189**, 35 (1972).
[46] N. M. Clarke, (1994) (unpublished).
[47] X. Chen, Y.-W. Lui, H. Clark, Y. Tokimoto, and D. H. Youngblood,Phys. Rev. **C 80**, 014312 (2009).
[48] A. H. Al-Ghamdi and Awad A. Ibraheem, Braz J Phys **46**, 334 (2016).
[49] Zakaria M. M. Mahmoud1, Kassem O. Behairy, Braz J Phys **47**, 189 (2017).
[50] S. R. Mokhtar, Awad A. Ibraheem , Eman Abdel-Rahman, M. El-Azab Farid, submitted to Prog. Theo. Exp. Phys., Japan.

دراسة التشتت المرنى للنواة الليثيوم ٦ والماغنيسيوم ٢٤ باستخدام صور مختلفة لنموذج الطى

شريف رشاد مختار ، عوض احمد ابراهيم ، ايمان عبد الرحمن احمد ومحمد العزب فريد
قسم الفيزياء جامعة اسيوط
قسم الفيزياء جامعة الازهر فرع اسيوط

في هذة الدراسة نقوم بدراسة التشتت المرن للتفاعل الاتي ^{6}Li+^{24}Mg للنواة المتصادمة $\alpha-$cluster
عند الطاقتين 88و٢٤٠ مليون الكترون فولت في اطار النموذج البصري . باستخدام نموذجين مختلفين وهما Sao_ paulo ,DFC ويعتمد الجزء الحقيقي للنموذجين علي التركيب العنقودي($\alpha-$cluster) للانوية المتصادمة . بالنسبة للجزء الحقيقي لنموذج الطي المزدوج يشتق بواسطة الطي علي التفاعل الفعال $\alpha-\alpha$ و $n-\alpha$ بين نواة القذ يفة والهدف من خلال التركيب العنقودي لنواة الماغنسيوم ونتعامل في هذة النموذج مع مكونات نواة الليثيوم وهما الفا والديترون ويسمي هذا النموذج بنموذج الطي المزدوج العنقودي . والنموذج الثاني هو عبارة عن جهد الطي المزدوج البصري ويعتمد علي Sao_ Paulo .ناخذ الجزء التخيلي لجهد البصري في صورة الودزو ساكسون بالنسبة للنموذج الطي المزدوج العنقودي ، بالنسبة ساوبولو في صورة الودزو ساكسون وفي صورة الجهود الطي التخيلي .وكلا النموذجين اعطي توافق مع الداتا العملية المقاسة ولاحظنا ان قيمة N_R تقترب من الواحد الصحيح .